Journal of Experimental Nanoscience

Publication details, including instructions for authors and subscription information:
http://www.informaworld.com/smpp/title~content=t716100757

Developing PbSe/PbS core-shell nanocrystals quantum dots toward their potential heterojunction applications

Dehu Cui[a]; Jian Xu[a]; Gary Paradee[a]; Shengyong Xu[b]; Andrew Y. Wang[c]
[a] Department of Engineering Science, Penn State University, State College, PA 16802, USA [b] Department of Physics, Penn State University, State College, PA 16802, USA [c] Ocean NanoTech, Fayetteville, AR 72701, USA

To cite this Article Cui, Dehu , Xu, Jian , Paradee, Gary , Xu, Shengyong and Wang, Andrew Y.(2007) 'Developing PbSe/PbS core-shell nanocrystals quantum dots toward their potential heterojunction applications', Journal of Experimental Nanoscience, 2: 1, 13 — 21

To link to this Article: DOI: 10.1080/17458080600935590

URL: http://dx.doi.org/10.1080/17458080600935590

Journal of Experimental Nanoscience,
Vol. 2, Nos. 1–2, March–June 2007, 13–21

Taylor & Francis
Taylor & Francis Group

Developing PbSe/PbS core-shell nanocrystals quantum dots toward their potential heterojunction applications

DEHU CUI†, JIAN XU*†, GARY PARADEE†, SHENGYONG XU‡
and ANDREW Y. WANG§

†Department of Engineering Science, Penn State University, State College, PA 16802, USA
‡Department of Physics, Penn State University, State College, PA 16802, USA
§Ocean NanoTech, LLC, Fayetteville, AR 72701, USA

(*Received June 2006; in final form July 2006*)

We report in this article the epitaxial growth of PbS shells over PbSe nanocrystal quantum dots (NQDs) with monolayer-precision. The core-shell infrared NQDs were ligand-exchanged with short-chain octylamine, and the photoluminescence efficiency of the surface-engineered core-shell nanoparticles was substantially higher than that of the plain-core structures undergoing the same surface processing, which reveals less ligand-dependence and enhanced chemical robustness in the core-shell NQDs. The reported results could potentially open up the possibility of incorporating semiconductor infrared NQDs in the silicon matrix to develop all-inorganic light emitting heterojunctions on silicon substrates.

Keywords: colloidal nanocrystals; quantum dots; photoluminescence; infrared, light emitting devices

1. Introduction

The newly developed colloidal nanocrystals of IV-IV compounds are currently receiving widespread attention due to their unique electronic structures and superior optical properties [1–6]. The quantized electronic transitions in Pb(S,Se) nanocrystal quantum dots (NQDs) have been reported to provide size-tunable interband absorption and luminescence emission at a broad and technically important infrared wavelength range, spanning 0.8–4.0 µm [7]. Sharp exciton absorption features and high photoluminescence (PL) efficiency ($\sim$89%) of PbSe NQDs have been reported [8]. Tunable optical gain and amplified spontaneous emission have been observed from PbSe nanocrystal films [9]. Electroluminescence devices based on Pb(S,Se) NQDs were demonstrated recently with a size-tunable infrared emission between 1.0 and 2.0 µm, and high external quantum efficiencies up to 3% [10–12].

The emergence of the high-quality infrared NQDs also opens the possibility of incorporating semiconductor infrared NQDs in the silicon matrix to develop

---

*Corresponding author. Email: jianxu@engr.psu.edu

Journal of Experimental Nanoscience
ISSN 1745–8080 print/ISSN 1745–8099 online © 2007 Taylor & Francis
http://www.tandf.co.uk/journals
DOI: 10.1080/17458080600935590

all-inorganic light emitting heterojunctions on silicon substrates. Such a heterojunction will comprise layers of infrared quantum dots embedded at the interface of a silicon p–n junction to form the intrinsic active region of a light-emitting diode (LED). Since PbSe NQDs and the crystalline silicon form overlapping Type-I heterojunctions at the interface ($E_{gNQD} \leq 1.0\,eV$), the free-carrier injection into PbSe nanocrystals is energetically favored from the wider band-gap silicon cladding layers. Electrons and holes will be injected, via n- and p-regions of the silicon junction, into the embedded NQDs, where the radiative recombination leads to the excitonic emission with quantum-enhanced efficiency and size tunable wavelengths. Since silicon is largely transparent to the infrared light ($\lambda \geq 1100\,nm$), the heterojunction will transmit the infrared emission from the NQD-active region with low losses.

The NQD-silicon integration scheme is, however, hindered by the fact that the as-prepared PbSe nanoparticles are overcoated with a layer of oleate ligands which function to passivate the surface traps as well as keeping NQDs from agglomerating in organic solvents [13]. The long-chain nature of the surfactant molecules poses barriers to the free-carrier transport between the guest NQDs and the host silicon layer, and introduces structural defects at NQD-NQD and NQD-silicon interfaces [14]. The technique of ligand exchange could potentially provide the ultimate solution to this problem by replacing the long-chain ligands with conductive or 'good-leaving' molecules which are readily removed from NQD thin films by vacuum-heating, leaving a layer of surface-engineered NQDs for the subsequent overgrowth of the semiconductor capping layer [15]. Successful ligand-exchange processes have so far only been achieved on nanoparticles of core-shell architectures, such as CdSe/CdS and CdSe/ZnS core-shell NQDs of the visible emission wavelengths. The wider band-gap (Zn, Cd)S shells effectively passivate and protect the radiative CdSe cores during the 'ligand removal' process, whereas those NQDs of plain-core structures often lose their emissivity substantially due to the degradation of the unprotected surfaces in the reaction [16].

In this article we report the epitaxial growth of PbS shells over PbSe NQDs with monolayer precision. The core-shell infrared NQDs were ligand-exchanged with short-chain octylamine, and the photoluminescence efficiency of the surface-engineered core-shell nanoparticles was substantially higher than that of the plain-core structures undergoing the same surface processing, which reveals less ligand-dependence and enhanced chemical robustness in the core-shell NQDs. While there has been a report on the successful synthesis of PbSe/PbS NQDs, the tributylphosphine/trioctylphospine (TBP/TOP) surfactant-based synthetic approach reported by Brumer *et al.* produced PbSe NQDs of lower quantum-efficiency (~40%) than those prepared with oleate ligand-based approach (~85%) [17]. In addition, there was no disclosed information on the ligand dependence, chemical stability and processibility of the synthesized core-shell structures yet.

2. Sample preparation

In this study, PbSe NQDs of plain-core structures were synthesized following the noncoordinating solvent technique developed by Yu *et al.* [2]. The as-prepared PbSe nanostructures were stabilized with a capping layer of oleate molecules coordinated to the Pb atoms. High-resolution transmission electron images of the synthesized NQDs show well resolved regular lattice fringes without detectable stacking fault and other internal defects, indicating the single crystalline-domain in the nanoparticles. The interband absorption spectra of 6 nm-NQDs exhibit sharp excitonic absorption features which are discernable up to the second order. Room-temperature PL from the PbSe solution is strong and exhibits small stokes shifts, indicative of a dominant band-edge emission. The full-width-at-half-maximum (FWHM) bandwidth of the PL emission of 6 nm-NQDs is 158 nm.

The technique of successive ion layer adsorption and reaction (SILAR) [18], originally developed for the deposition of thin films on solid substrates from solution baths, was adapted to the growth of high-quality PbSe/PbS core-shell nanocrystals. While Li *et al.* [19] adopted such a synthetic approach to grow wider bandgap shells over II-VI NQDs with an impressive success, efforts were made to apply the SILAR technique to the IV-VI NQD system due to the different compound families and coordinating ligands involved in the synthesis. In order to gain the monolayer-control over the shell formation, cationic and anionic precursors, Pb^{2+} and S^{2-}, were injected alternatively into the reaction mixture with core nanocrystals. The dosage of each injection was precisely controlled such that one-half of a shell-monolayer will grow epitaxially over PbSe plain-cores following each addition of either cationic or anionic reagents. Since there was little opportunity for the cationic and anionic species to coexist with each other in the reaction solution, direct nucleation of the shell-compound into cores was avoided.

During the SILAR synthesis, highly fluorescent PbSe nanocrystals were first purified by mixing with bad solvent (acetone), centrifuge-precipitating and decantation. The PbSe nanocrystals were then diluted in Octadecene (ODE), heated to ~140°C in a three-neck flask. A lead-injection solution was prepared by mixing PbO, Oleic acid and ODE in the second three-neck flask, heated to ~157°C under the argon flow to obtain a colorless clear solution. The sulfur-injection solution was prepared by dissolving sulfur in TOP (trioctylphosphine) and ODE, then sonicating the mixture in ultrasonic bath to get a clear solution. The temperature of lead-injection solution was retained at ~80°C, whereas the sulfur-injection solution was allowed to cool to room temperature.

The shells were grown epitaxially, one monolayer at a time, by the consecutive syringe-injection of the pre-determined dosages of lead and sulfur solutions into the pre-heated PbSe-core solution using the standard air-free procedure. The amounts of lead and sulfur precursors required for the first shell-layer growth were determined by the size and the lattice structure of the PbSe plain-cores employed in the synthesis. The reaction temperature was kept at 140°C, below that required for the nucleation of individual PbS nanocrystals. To monitor the reaction, aliquots were taken 1–5 min after every two successive injections of lead and sulfur solutions for the absorption and PL measurements. When the desired number of shell layers was reached, the reaction mixture was cooled to terminate the reaction. In this approach PbSe/PbS NQDs of 1–5 shell layers have been synthesized. According the lattice constants of bulk PbS and PbSe crystals [20], there is a 3.1%-tensile strain in PbS-shell layers epitaxially grown over PbSe plain-cores. The calculated critical thickness substantially exceeds the thickness of five layers of PbS shells, which excludes the concern of any strain related dislocations in our investigation of II-VI core-shell structures.

3. Characterization and analysis

The final product was diluted by chloroform which was followed by a methanol extraction. Excess ligands were further removed by repeatedly precipitating the core-shell NQDs with acetone and eventually dispersed in chloroform for storage. A small portion of the nanocrystals were re-dispersed in tetrachloroethylene for NIR absorption and PL measurements. The PL spectroscopy of PbSe/PbS NQDs was characterized with a CM110 Spectralproducts NIR spectrometer and a 904 nm-diode laser module as the excitation source.

Figure 1 shows the evolution of PL spectra of the core-shell NQDs upon the growth of PbS shell in a typical reaction. A consistent red-shift of the peak wavelength was observed from the PL spectra upon the increase of the number of shell layers. Similar shifts of wavelength were also observed by Li *et al.* [19] and Dabbousi *et al.* [21] during their syntheses of CdSe/CdS core-shell NQDs. We believe that the increased layer number of PbS shells reduces the quantum confinement on the electronic transitions in PbSe cores due to the relatively low barrier height at PbSe/PbS interface (~0.1 eV) and renders the spreading of the carriers' wavefunctions out of the core regions, which in turn leads to the observed red shifts of the optical transition with respect to the plain-core samples. The intensity variation of the sample PL during the overgrowth of PbS shells exhibits an initial fall and the subsequent increment up to the third layer, which corresponds to 85% of the maximum quantum efficiency of plain-core PbSe NQDs. Upon the growth of thicker PbS shells, the PL intensity of the sample starts to decline again.

The epitaxial growth of the core/shell structures was verified by high resolution transmission electron microscopy. Well defined fringes are continuous throughout the entire particle, indicative of the epitaxial nature of the shell growth. In comparison with

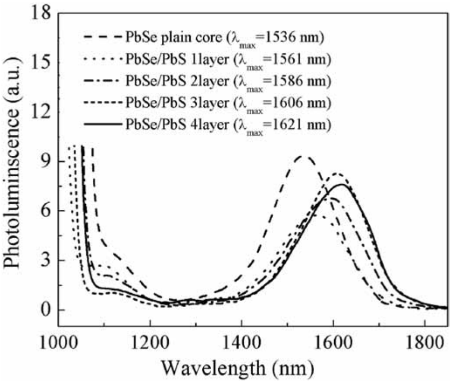

Figure 1. The evolution of the photoluminescence spectra of PbSe/PbS core-shell nanocrystals upon the growth of PbS shells in the chemical synthesis.

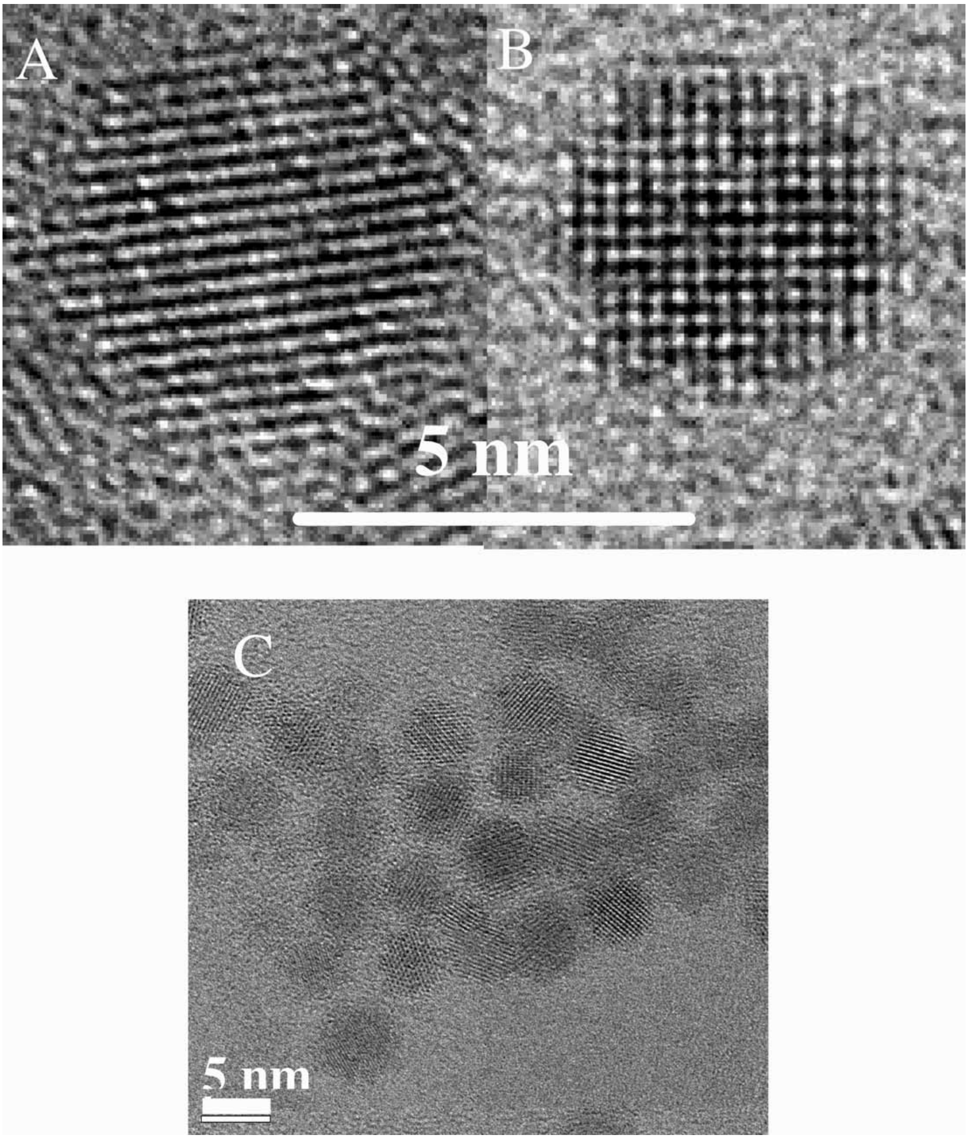

Figure 2. High resolution transmission electron microscopic images of PbSe nanocrystals (left) with and (right) without the overcoating of PbS shells (of four monolayers).

spherical NQDs of plain-core structures, the core-shell PbSe NQDs exhibit larger size with slightly elongated shape. While monodispersed plain-core NQDs often form well ordered 2D-superlattices when they are deposited from solutions by the controlled evaporation, the elongated core-shell NQDs tend to align randomly regarding to each other and lack long range orders in the thin film. This is reflected by the blurring of the diffraction rings in the selected-area-electron-diffraction (SAED) patterns of core-shell nanocrystals revealing the misorientation of the c-axes in the deposited

Figure 3. Selected-area-electron-diffraction (SAED) patterns of plain-core PbSe (upper half) and core-shell PbSe/PbS nanocrystals (lower half).

nanoparticle-thin films (figure 3). The same trend was also reported for II-VI core-shell NQDs [19, 21]. The observed aspect ratio in the NQD shape upon multi-layer shell coverage is possibly due to the preferred shell growth along certain crystal directions when the shell thickness is beyond a critical number of atomic layers.

X-ray Photoelectron Spectroscopy (XPS) analysis on the core-shell NQDs was performed on a modified Kratos XSAM 800 pci using Mg Kα radiation (1253.6 eV) with an x-ray voltage of 12 kV, a current of 20 mA, and a pass-energy of 20 eV. The XPS data was collected in high resolution mode with a step size of 0.2 eV with dwell times varying to obtain a reasonable signal to noise ratio. Both plain-core PbSe nanocrystals and nanocrystals overcoated by four monolayers of PbS shells were examined by XPS. It has been found that both Se_{3P} and S_{2P} peaks are detectable in the XPS spectrum of core-shell structures, whereas only the Se_{3P} peak appears in the spectrum of bare dot structure. This, again, confirms the overcoating of the selenium compound core with the sulfide based shell layer.

The processibility of the core-shell NQDs was investigated by conducting ligand exchange on the nanocrystal surfaces and studying the photoluminescence properties of the surface-engineered core-shell nanoparticles in comparison with their plain-core counter parts. While the oleate ligand based synthetic approach has been developed to produce IV-VI infrared NQDs of high quantum efficiency, the long chain nature of the '18-carbon' oleic molecules poses barriers for the charge separation and the

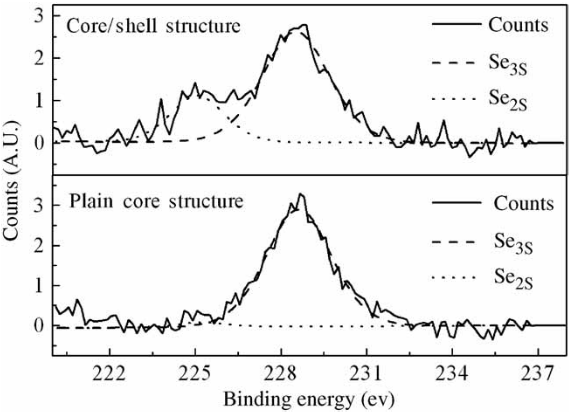

Figure 4. XPS spectra of plain-core PbSe (lower half) and core-shell PbSe/PbS nanocrystals (upper half).

carrier-transport at the nanocrystal surface, which substantially limit the applications of these infrared NQDs in LED and photovoltaics [11, 22, 23]. Techniques such as ligand exchange and ligand removal are under investigation in order to address this problem, and the core-shell architecture of NQDs could potentially protect the light sensitive cores from degrading when undergoing post-synthesis chemical treatments. In our study, the oleic acid molecules overcoating the core-shell NQDs have been replaced with short-chain '8-carbon' octylamine molecules to investigate the effect of the shell layer on the optical properties of the ligand exchanged NQDs.

The detail of the ligand exchange process is described as follows [24]. The powder of as-prepared PbSe nanocrystals was first prepared from the solution with the methanol precipitation, centrifugation, decantation and drying processes. The precipitated nanocrystal powder was then dissolved in a small amount of octylamine ($C_8H_{19}N$). After the solution was heated at 75°C for 16 h, and the octylamine-capped nanocrystals were immediately purified from the excess ligands by precipitation with a polar solvent, and the final precipitate was dispersed into the desired solvent for storage. Some plain-core PbSe NQDs were also ligand-exchanged with the same procedure and used as control samples in our study. The ^1H NMR spectroscopy (Bruker AM 300, $CDCl_3$ as solvent) was used to identify the ligand exchange process of PbSe/PbS NQDs. Oleic acid-capping of the as-prepared core-shell NQDs was confirmed by the presence of the peak around 5.3 ppm due to -HC=CH- segments in oleate molecules (figure 5a). After ligand-exchange with octylamine, the peak at 5.3 ppm completely disappears and a new peak at ~2.0 ppm shows up corresponding to the primary amine group of octylamine (figure 5b). This provides the evidence that oleic acid bound to PbSe/PbS nanocrystals has been successfully removed and replaced with the octylamine ligand.

PL characterization on the ligand exchanged PbSe/PbS core-shell NQDS has revealed a peak-intensity drop of ~36% with respect to the as-synthesized core-shell ones without noticeable wavelength shift of the PL maxima. In contrast, the PL yield of the control samples, i.e. the plain-core PbSe NQDs, dropped by 90% after the treatment of the ligand exchange, which was also accompanied by a slight blue-shift (~5 nm) of the PL maximum. A similar decrease of the quantum yield were observed in

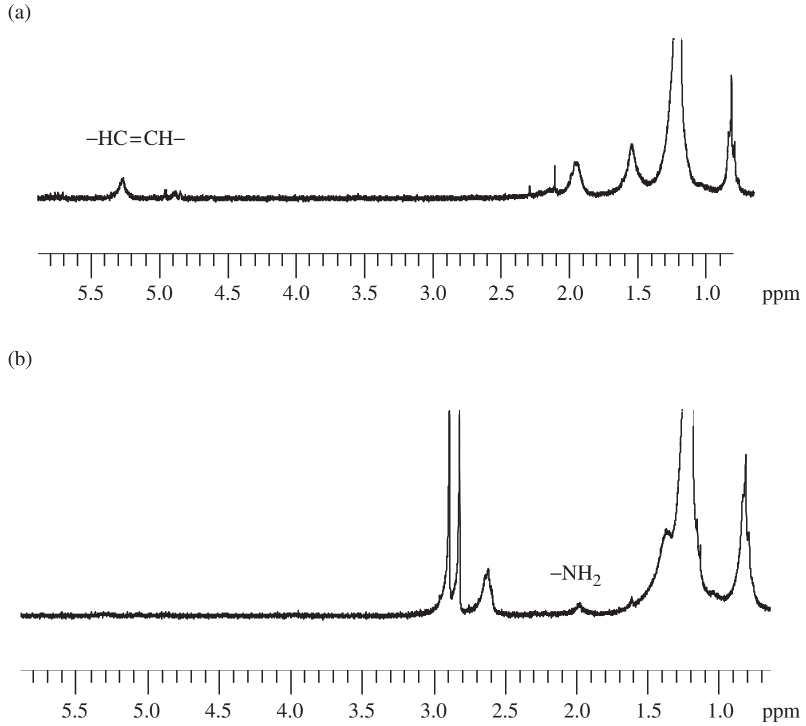

Figure 5. 1H NMR spectra of (a) as — prepared PbSe/Pbs NQDs dispersed in $CDCl_3$ and (b) ligand-exchanged NQDs dispersed in $CDCl_3$.

ligand-exchanged CdSe NQDs and has been attributed to a loss of passivation on the surface of the QD which creates new defects and opens up pathways for nonradiative relaxation [16, 19, 21]. The fact that the core-shell infrared NQDs exhibit less reduction of the photoluminescence efficiency than the plain-core structures after undergoing the same ligand exchange process clearly indicates that the light-emitting core in the core-shell architecture are better protected by the wide band gap semiconductor shells and therefore, more robust toward the subsequent chemical/physical treatments in their electronic/optoelectronic device applications.

Acknowledgment

J. Xu would like to thank Dr Thomas E. Mallouk, DuPont Professor of Materials Chemistry and Physics at the Penn State University, for the experimental help on the synthesis of semiconductor nanocrystals. The authors also thank Dr Michael Gerhold for helpful discussions on the device applications of PbSe NQDs. This work was supported by the US Army Research Office under Contract No. DAAD19-02-D-0001, and by the National Science Foundation of USA under grant DMR-0213623.

References

[1] B.C. Murray, S. Sun, W. Gaschler, H. Doyle, A.T. Betley, R.C. Kagan. Colloidal synthesis of nanocrystals and nanocrystal superlattices. *IBM J. Res. Dev.*, **45**, 47 (2001).

[2] W.W. Yu, C.J. Falkner, S.B. Shih, L.V. Colvin. Preparation and characterization of monodisperse PbSe semiconductor nanocrystals in a noncoordinating solvent. *Chem. Mater.*, **16**, 3318 (2004).

[3] C. Feng, L.K. Stokes, W. Zhon,, J. Fang, B.C. Murray. Synthesis and properties of lead selenide nanocrystal solids. Proceedings of the Materials Research Society Symposium, **691**, 359 (2002).

[4] A.M. Hines, D.G. Scholes. Colloidal PbS nanocrystals with size-tunable near-infrared emission: observation of post-synthesis self-narrowing of the particle size distribution. *Adv. Mater.*, **15**, 1844 (2003).

[5] L.B. Wehrenberg, W. Congjun, P. Guyot-Sionnest. Interband and intraband optical studies of PbSe colloidal quantum dots. *J. Phy. Chem. B.*, **106**, 10634 (2002).

[6] K.U. Gautam, R. Seshadri. Preparation of PbS and PbSe nanocrystals by a new solvothermal route. *Mater. Res. Bull.*, **39**, 669 (2004).

[7] M.J. Pietryga, D.R. Schaller, D. Werder, H.M. Stewart, I.V. Klimov, A.J. Hollingsworth. Pushing the band gap envelope: Mid-infrared emitting colloidal PbSe quantum dots. *J. Am. Chem. Soc.*, **126**, 11752 (2004).

[8] H. Du, C. Chen, R. Krishnan, D.T. Krauss, M.J. Harbold, W.F. Wise, G.M. Thomas, J. Silcox. Optical properties of colloidal PbSe nanocrystals. *Nano Lett.*, **2**, 1321 (2002).

[9] D.R. Schaller, A.M. Petruska, I.V. Klimov. Tunable near-infrared optical gain and amplified spontaneous emission using PbSe nanocrystals. *J. Phys. Chem. B.*, **107**, 13765 (2003).

[10] S.J. Steckel, S. Coe-Sullivan, V. Bulovic, G.M. Bawendi. 1.3 μm to 1.55 μm tunable electroluminescence from PbSe quantum dots embedded within an organic device. *Adv. Mater.*, **15**, 1862 (2003).

[11] E.H. Sargent. Infrared quantum dots. *Adv. Mater.*, **17**, 515 (2005).

[12] B.L. Wehrenberg, P. Guyot-Sionnest. Electron and hole injection in PbSe quantum dot films. *J. Amer. Chem. Soc.*, **125**, 7806 (2003).

[13] D.S. Ginger, N.C. Greenham. Charge injection and transport in films of CdSe nanocrystals. *J. Appl. Phys.*, **87**, 1361 (2000).

[14] C.B. Murray, C.R. Kagan, M.G. Bawendi. Synthesis and characterization of monodisperse nanocrystals and close-packed nanocrystal aassemblies. *Annu. Rev. Mater. Sci.*, **30**, 545 (2000).

[15] M. Danek, K.F. Jensen, C.B. Murray, M.G. Bawendi. Electrospray organometallic chemical vapor deposition—A novel technique for preparation of II–VI quantum dot composites. *Appl. Phys. Lett.*, **65**, 1368 (1994).

[16] M. Kuno, J.K. Lee, B.O. Dabbousi, F.V. Mikulec, M.G. Bawendi. The band edge luminescence of surface modified CdSe nanocrystallites: Probing the luminescing state. *J. Chem. Phys.*, **106**, 646 (1997).

[17] A. Sashchiuk, L. Langof, R. Chaim, E. Lifshitz. Synthesis and characterization of PbSe and PbSe/PbS core–shell colloidal nanocrystals. *J. Crys. Growth*, **240**, 431 (2002).

[18] S. Park, B.L. Clark, D.A. Keszler, J.P. Bender, J.F. Wager, T.A. Reynolds, G.S. Herman. Low-temperature thin-film deposition and crystallization. *Science*, **297**, 65 (2002).

[19] J.J. Li, A. Wang, W. Guo, J.C. Keay, Tetsuya, D. Mishima, M.B. Johnson, X. Peng. Large-scale synthesis of nearly monodisperse CdSe/CdS core/shell nanocrystals using air-stable reagents via successive IO layer adsorption and reaction. *J. Am. Chem. Soc.*, **125**, 12567 (2003).

[20] M. Shur. *Physics of semiconductor devices*, 1st ed., Prentice Hall, New York, USA (1990).

[21] B.O. Dabbousi, J. Rodriguez-Viejo, F.V. Mikulec, J.R. Heine, H. Mattoussi, R. Ober, K.F. Jensen, M.G. Bawendi. (CdSe)ZnS core-shell quantum dots: synthesis and characterization of a size series of highly luminescent nanocrystallites. *J. Phys. Chem. B*, **101**, 9463 (1997).

[22] D. Cui, J. Xu, S. Xu, G. Paradee, B. A. Lewis, and M. Gerhold. Infrared photodiode based on colloidal PbSe nanocrystal quantum dots, *IEEE T. Nanotech*, **5**, 1 (2006).

[23] D. Cui, J. Xu, T. Zhu, G. Paradee, S. Ashok, M. Gerhold. Harvest of near infrared light in PbSe nanocrystal-polymer hybrid photovoltaic cells. *Appl. Phys. Lett.*, **88**, 183111 (2006).

[24] D. Cui, J. Xu, G. Paradee, Q. Wang. Ligand dependences of the infrared responses of colloidal PbSe nanocrystal quantum dots (in preparation).